coatings

MDPI

Article

Localized Corrosion Mechanism of Q125 Casing Steel in Residual Acid Solution during Oil Reservoir Acidizing

Wei Yan [1,*], Zelin Ma [1], Zhi Wang [1], Jingru Zhang [1], Kepei Li [1], Lei Wen [2], Chen Li [3], Xiaohui Jiang [1] and Zhengxian Xu [1]

[1] State Key Laboratory of Oil and Gas Resources and Detection, China University of Petroleum, Beijing 102249, China
[2] National Center for Materials Service Safety, University of Science and Technology Beijing, Beijing 100083, China
[3] College of Mechanical Engineering, Guangxi University, Nanning 530004, China
* Correspondence: yanwei@cup.edu.cn

Abstract: This paper aims to investigate the localized corrosion mechanism of Q125 casing steel in residual acid solution with Mannich base type inhibitors during oil reservoir acidizing process. The corrosion behavior of Q125 casing steel in fresh acid (20% HCl) and residual acid solution (pH 1.0 and pH 3.0 HCl) with and without 3-(4-chlorophenylimino)-1-(piperidine-1-ylmethyl) indolin-2-one (Mannich base type, Mb) inhibitor was studied by electrochemical test, weight loss, and surface analysis. The morphology and composition of corrosion products were analyzed by SEM/EDS and XPS; the local corrosion rate of casing steel with or without inhibitor was obtained by 3D profilometry. It was determined that the inhibitor had higher inhibition efficiency in fresh acid conditions than in residual acid conditions. Under the condition of residual acid, the decrease in inhibitor molecular coverage on the substrate surface promotes the occurrence of local corrosion. Pitting corrosion was detected in the residual acid solution containing Mannich base inhibitor, which may be related to the fact that $FeCO_3$ hinders the adsorption of inhibitor molecules on the substrate surface.

Keywords: Q125 casing steel; corrosion; mannish base inhibitor; acidizing fracturing; localized corrosion

check for updates

Citation: Yan, W.; Ma, Z.; Wang, Z.; Zhang, J.; Li, K.; Wen, L.; Li, C.; Jiang, X.; Xu, Z. Localized Corrosion Mechanism of Q125 Casing Steel in Residual Acid Solution during Oil Reservoir Acidizing. *Coatings* **2023**, *13*, 710. https://doi.org/10.3390/coatings13040710

Academic Editors: Marin Kurtela and Ajay Vikram Singh

Received: 14 February 2023
Revised: 17 March 2023
Accepted: 27 March 2023
Published: 31 March 2023

Copyright: © 2023 by the authors. Licensee MDPI, Basel, Switzerland. This article is an open access article distributed under the terms and conditions of the Creative Commons Attribution (CC BY) license (https://creativecommons.org/licenses/by/4.0/).

1. Introduction

Q125 casing steel is a highly specialized type of steel that is widely used in the oil and gas extraction industry due to its exceptional strength, toughness, and corrosion resistance [1]. The harsh environmental conditions, such as high temperatures, high pressures, and corrosive substances, make it essential for the materials used in these applications to possess excellent corrosion resistance and high strength. However, despite its outstanding properties, Q125 casing steel can still suffer from severe corrosion damage, particularly in acidic environments [2]. Therefore, developing effective corrosion protection measures to improve the material's resistance to corrosion is crucial.

As the demand for oil and gas continues to increase, there has been a growing emphasis on efficient and sustainable extraction methods [3–5]. Acid fracturing technology is one such method that can enhance reservoir permeability and improve oil recovery rates [6,7]. However, the process of acidification in a tubing string can lead to corrosion of the metal materials due to the chemical reaction between the acid and the metal [8,9]. This is particularly true for high temperature acidification systems, where hydrochloric acid with a mass fraction of 20% or greater is commonly used as the base fluid. To address this issue, the simplest and most effective approach is to add corrosion inhibitors to the acid solution [4,10–12]. In this regard, the Mannich base type corrosion inhibitors are widely used in acid fracturing due to their high corrosion inhibition efficiency and low toxicity [13]. Therefore, understanding the corrosion resistance properties of Q125 casing steel and the use of corrosion inhibitors is crucial for the efficient and sustainable extraction of oil and gas.

Mannich base type corrosion inhibitor is mainly obtained by the condensation reaction of ketone, aldehyde, and amine containing active hydrogen. The synthesis methods of Mannich base corrosion inhibitors are diverse, the molecular structures of the obtained corrosion inhibitors are different, and the corrosion inhibition effects of the Mannich base corrosion inhibitor molecules with different structures are also different. Ahamad et al. [14] studied the inhibition efficiency of four piperidinylmethylindoline-2-one derivatives in 1 M HCl solution. It was determined that the different substituents of the aniline group would affect the inhibition efficiency. Furthermore, Ahamad et al. [14] reported that the lower the energy of the HOMO (highest occupied molecular orbital), LUMO (lowest unoccupied molecular orbital), and HOMO-LUMO gaps of the corrosion inhibitor, the higher the inhibition efficiency of the corrosion inhibitor. The results of Ayeni et al. [13] and Ferkous et al. [15] also support this view. Pan et al. [16] studied the effect of hydrophobic group carbon chain length on the corrosion inhibition efficiency of N80 steel in 15% HCl solution and determined that when the inhibitor content was less than 0.6%, the Mannich base inhibitor with short carbon chain had better corrosion inhibition performance. Guo et al. [17] synthesized a double Mannich base inhibitor using N-octylamine, acetophenone, and formaldehyde as the main raw material and reported that a double Mannich base inhibitor compared to a single Mannich base corrosion inhibitor had higher corrosion inhibition efficiency.

However, most of the above studies focused on the inhibition effect of inhibitors under fresh acid conditions. Fresh acid reacts with alkaline ore to obtain residual acid, and the pH value of residual acid is higher than that of fresh acid. However, the effect of residual acid and residual carbonate products on the corrosion inhibition efficiency of inhibitors is not clear. Therefore, investigation of the effects of Mb on the corrosion behaviors of Q125 casing steel in fresh and residual acid solutions can not only reveal the internal causes of string failure, but also provide certain guiding significance for the development of low permeability reservoirs and reservoir reconstruction projects.

2. Materials and Methods

2.1. Materials and Pretreatment

The chemical composition of Q125 grade casing steel used in this experiment is 0.28 C, 0.29 Si, 0.55 Mn, 0.98 Cr, 0.31 Mo, 0.03 Nb, 0.15 V, 0.006 P, 0.002 S, and Fe in balance (wt.%). The exposed area of the working electrode is 10 mm × 10 mm; the sample size of weight loss test is 30 mm × 10 mm × 3 mm. Before the experiment, all the samples were ground to 600 mesh by SiC sandpaper step by step. The oil was deoiled with acetone, then dehydrated by ethanol, and placed in a vacuum drying oven for 24 h.

2.2. Test Procedures

The experiment was carried out in a 2 L glass cell. Three-electrode system was used in the electrochemical test. A saturated calomel (Hg/Hg_2Cl_2, SCE) reference electrode was connected by a lugin capillary tube, and the counter electrode was a platinum electrode. The pH value of the solution was measured by a pH electrode (METTLER TOLEDO, FE20, Columbus, OH, USA). A potentiostat was used for the electrochemical test (GAMRY, Reference 3000, Warminster, PA, USA). The experiment was carried out in the solution of residual acid and fresh acid with or without 1 wt.% Mb at atmosphere pressure and 90 °C. The chemical structure of the Mb corrosion inhibitor (Provided by the Beijing Comers Oilfield Chemicals Technology Co., Ltd., Beijing, China: MB-CS125) is shown in Figure 1.

When the electrode was immersed in the solution for 4 h, the electrochemical test was carried out. The polarization range of the polarization resistance was relative to the open circuit potential (OCP) ± 10 mV, and the scan rate was 0.125 mV s^{-1}.The test range of potentiodynamic scanning was ±200 mV, and the scanning rate was 0.2 mV s^{-1}. The dynamic potential scan first performed cathodic polarization, and when the polarization returned to OCP after the end of the polarization, the anode polarization scan was performed.

EIS was carried out in the range of open circuit potential ±5 mV, and the frequency range was 10^4 Hz to 10^{-2} Hz.

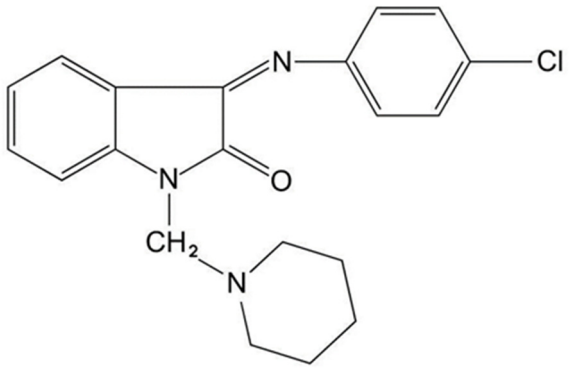


Figure 1. Chemical structure of Mb.

After the electrochemical test, the weight loss method specimens were immersed in the test solution for 4 h to study the influence of Mannich base type corrosion inhibitor on the corrosion behavior of Q125 grade casing steel under the conditions of fresh acid and residual acid. The corroded samples were cleaned with deionized water and dehydrated with ethanol. The corrosion products were removed from the corrosion samples by using Clark solution (50 g stannous chloride, 20 g antimony trioxide, and concentrated chlorogenic acid per 1000 mL) according to the standards of the American Society for Testing and Materials (ASTM) [18], and then dried weighed by an electronic balance. The corrosion rate was obtained by weight loss method according to Formula [19], and the inhibition efficiency is expressed in Formula (2):

$$V = \frac{W_0 - W}{S \times t} \quad (1)$$

$$Inhibition\ efficiency = \frac{V_0 - V_m}{V_0} \times 100\%, \quad (2)$$

where V is the corrosion rate, g m^{-2} h^{-1}; W_0 is the weight of the sample before corrosion, g; W is the mass of the sample after corrosion, g; S is the surface area of the sample, m^2; t is immersion time, h; V_0 is the corrosion rate without inhibitor, g m^{-2} h^{-1}; V_m is the corrosion rate with inhibitor, g m^{-2} h^{-1}.

The surface morphology was analyzed by Scanning Electron Microscope (SEM)/Energy Dispersive Spectrometer (EDS). The local corrosion was analyzed by three-Dimension (3D) topography. The components of corrosion products were analyzed by X-ray Photoelectron Spectroscopy (XPS), and the spectra were fitted by XPS peak software.

3. Results

3.1. Uniform Corrosion Rate

Figure 2 shows the weight loss results of casing steel in fresh and residual acid solutions with and without Mb inhibitor. The study determined that when there was no Mb inhibitor, the corrosion rate decreased as the hydrogen ion concentration in the solution decreased. However, even when the pH of the solution was 3.0, the casing steel still had a higher corrosion rate of 92.48 g m^{-2} h^{-1}. When Mb appeared, Mb could effectively inhibit the occurrence of uniform corrosion of casing steel. Although the corrosion inhibition efficiency decreased slightly as the hydrogen ion concentration of the solution decreased, it still had a higher corrosion inhibition effect, and the corrosion inhibition efficiency was 98.8% under the condition of pH 3.0.

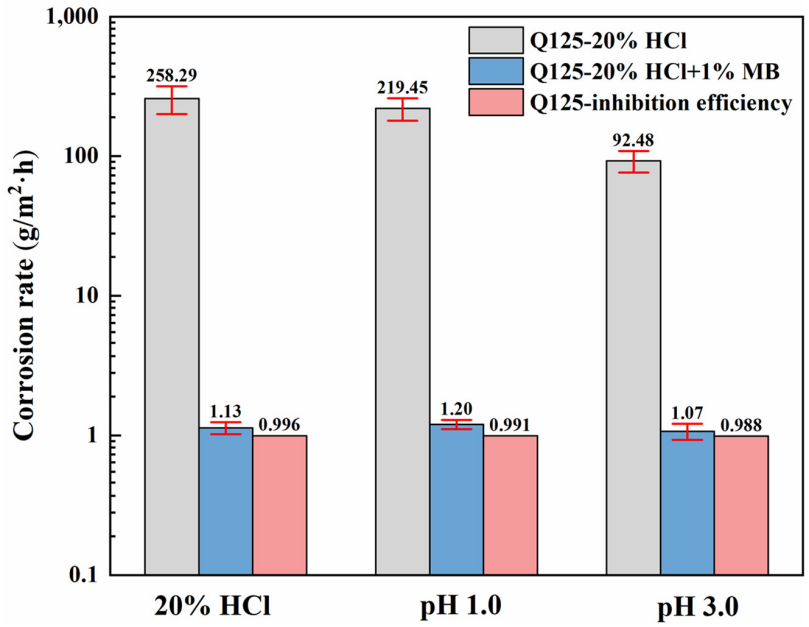


Figure 2. Uniform corrosion rate of casing steel immersed in fresh and residual acid solutions with or without Mb inhibitor for 4 h at 90 °C.

3.2. Electrochemical Measurements

The polarization curves of casing steel in fresh and residual acid solutions with and without Mb inhibitor for 4 h are shown in Figure 3. Under the condition of fresh acid, the appearance of Mb inhibited the anodic reaction and cathodic reaction of casing steel. The appearance of Mb caused the OCP to move up. Under the condition of residual acid, the OCP was significantly lower than that under the condition of fresh acid, and with the decrease in hydrogen ion content, the OCP decreased. When the corrosion inhibitor appeared, it could also inhibit the anode process and cathode reaction process, and the appearance of the corrosion inhibitor caused the OCP to move up, which was the same as that in the fresh acid condition, but the cathode reaction process in the residual acid condition was controlled by activation and diffusion. Compared with the condition of pH 3.0, the inhibition effect of Mb on the anodic reaction was more obvious at pH 1.0.

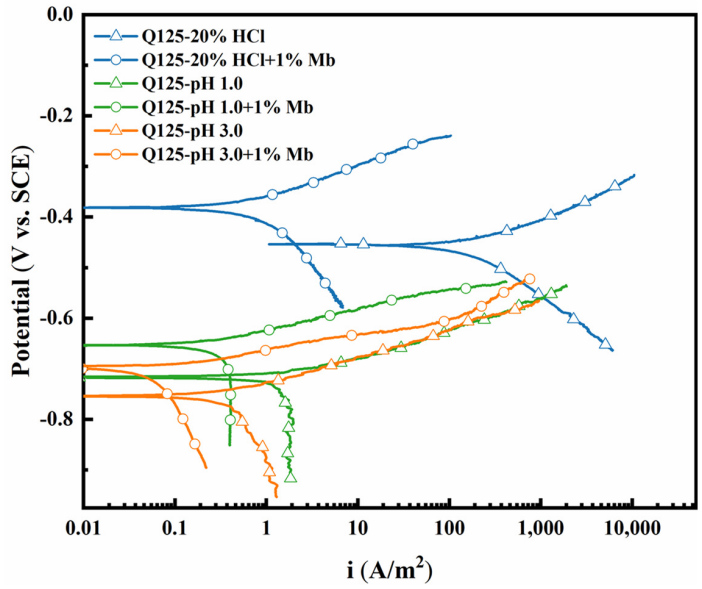


Figure 3. Polarization curves of casing steel immersed in fresh and residual acid solutions with or without Mb inhibitor for 4 h at 90 °C.

Table 1 presents the results of fitting electrochemical parameters obtained from potentiodynamic polarization curves recorded under various conditions depicted in Figure 3, where b_a is the anode Tafel slope, b_c is the cathode Tafel slope, r_p is the resistance of polarization, E_{corr} is the corrosion electrode potential, i_{corr} is the corrosion current density. Under residual acid conditions (pH 1.0 and pH 3.0), the cathode had a large Tafel slop. This phenomenon occurred because a large amount of $CaCO_3$ was added to the fresh acid (20% HCl) to neutralize the strong acid to obtain the residual acid solution. The addition of a large amount of $CaCO_3$ affected the chemical environment of the solution phase and thus the cathode reaction process. Moreover, the addition of Mb increased the Tafel slope of the anode and cathode compared with the fresh acid and residual acid without Mb. The trend of corrosion current density obtained by electrochemical test is consistent with the trend of corrosion current density obtained by weight loss method, showing significant attenuation characteristics. In addition, in terms of polarization resistance, it can also be seen that the addition of Mb inhibitor greatly increases the electrochemical corrosion resistance. Ferreira et al. [20] reported that when the displacement of E_{corr} was greater than 85 mV when the corrosion inhibitor appeared, the corrosion inhibitor belonged to the anodic or cathodic inhibition effect. When the displacement of the E_{corr} is less than 85 mV, the corrosion inhibitor is in a mixed inhibition effect. It could be seen from Table 1 that under the conditions of residual acid and fresh acid, the corrosion inhibitor has a mixed inhibitory effect.

Table 1. The fitting results of potentiodynamic polarization curve parameters under different conditions.

Condition	b_a mV/dec	b_c mV/dec	r_p	E_{corr}/mV	i_{corr}/mA cm^{-2}
20% HCl	61.55	95.24	8.2	−453.2	1.60
20% HCl + Mb	66.19	126.2	232.1	−381.2	0.081
pH 1.0	43.78	511	42.1	−717.2	0.42
pH 1.0 + Mb	47.02	548.7	463.3	−652.7	0.041
pH 3.0	51.56	235.5	140.1	−753.6	0.13
pH 3.0 + Mb	54.69	251.9	524.2	−694.7	0.037

Figure 4 shows the EIS results of casing steel under different conditions. When no Mb was added, the impedance spectrum exhibited a time constant, Figure 4b. When Mb was added, the impedance spectrum exhibited two (20% HCl + Mb and pH 1.0 + Mb, Figure 4c) or three (pH 3.0 + Mb, Figure 4d) time constants. The capacitive reactance arc in the high frequency region may be attributed to double layer capacitance. The capacitive arc in the middle- and low-frequency regions may be attributed to the corrosion product film or the adsorption film formed on the substrate surface by Mb. The inductive loop in the low-frequency region may be due to the adsorption process of Mb molecules. Under the same pH value, the diameter of the semicircular capacitor arc increases obviously when corrosion inhibitors appear, which indicates that Mb inhibited the progress of corrosion and reduced the corrosion rate.

Three kinds of equivalent circuit diagrams are shown in Figure 5 and the corresponding EIS fitting results are shown in Table 2 to demonstrate the obtained electromechanical parameters within different experimental conditions. Figure 5a was used to fit the EIS data of fresh acid and residual acid without Mb. Figure 5b was used to fit the EIS data of fresh acid and pH 3.0 with Mb (two time constants), and Figure 5c was used to fit the EIS data of pH 1.0 with Mb (three time constants). In the equivalent circuit diagram, Q_{dl} is the constant phase angle element representing double-layer capacitance; R_{ct} is charge transfer resistance; Q_f is the constant phase angle element representing the capacitance of the corrosion product film or the adsorption film formed by Mb. R_f is the resistance of the corrosion product film or the adsorption film formed by Mb; L and R_L represent inductance and inductive resistance, respectively; n_{dl} and n_f are the constant phase angle element exponents. With the increase in pH value, the impedance (R_{ct} + R_f) increased, indicating that the corrosion rate decreased with the increase in pH value without Mb. When Mb

was added, compared with the same pH value without Mb, the impedance value at least doubled, indicating that Mb could significantly reduce the corrosion rate. When Mb was added to fresh acid, the proportion of impedance value increased most, indicating that the inhibitor had the highest inhibition efficiency under fresh acid conditions.

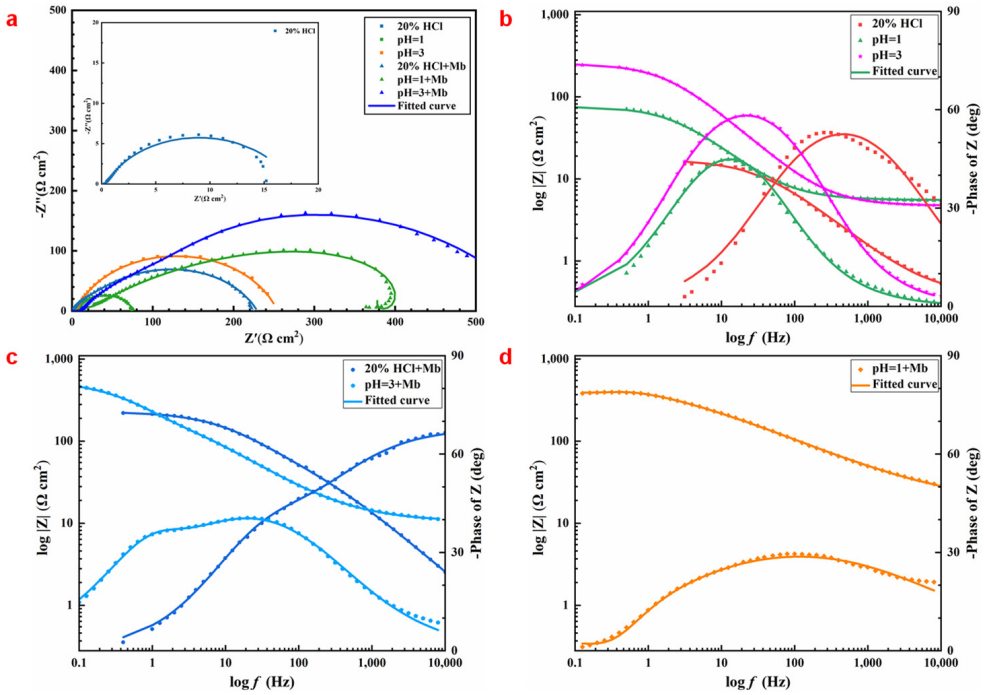


Figure 4. EIS of casing steel immersed in fresh and residual acid solutions with or without Mb inhibitor for 4 h at 90 °C. (**a**) Nyquist diagram; (**b**–**d**) Bode diagram.

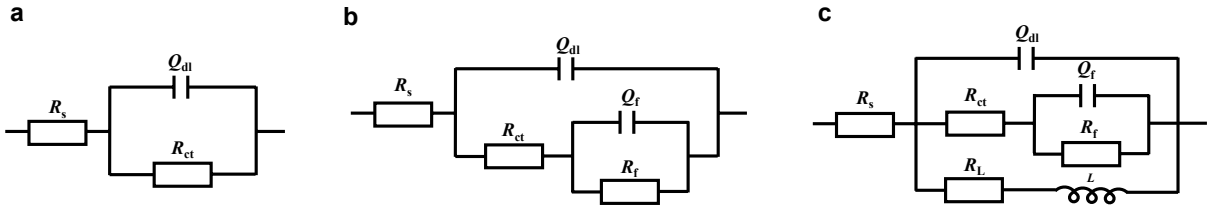


Figure 5. Fitting circuit of EIS results in Figure 4. Note: (**a**) 20% HCL, pH = 1, and pH = 3; (**b**) 20% HCL + Mb and pH = 3 + Mb; (**c**) pH = 1 + Mb.

Table 2. Fitting parameters of EIS of casing steel immersed in fresh and residual acid solution with or without Mb inhibitor for 4 h.

Condition	Q_{dl} (Ω^{-1} cm^{-2} s^{-ndl})	n_{dl}	R_{ct} (Ω cm^2)	Q_f (Ω^{-1} cm^{-2} s^{-ndl})	n_f	R_f (Ω cm^2)	L (H cm^{-2})	R_L (Ω cm^2)
20% HCl	9.67×10^{-5}	0.75	16.74					
20% HCl + Mb	9.34×10^{-4}	0.75	76.95	1.8×10^{-4}	0.74	151.7		
pH 1.0	1.57×10^{-3}	0.8	69					
pH 1.0 + Mb	3.93×10^{-7}	0.93	14.35	4.76×10^{-4}	0.48	504.7	1541	1188
pH 3.0	5.56×10^{-4}	0.8	250.9					
pH 3.0 + Mb	8.64×10^{-4}	0.61	330.2	6.89×10^{-4}	1	240.5		

3.3. Surface Morphology Analysis

Figure 6 shows the SEM results of casing steel in fresh and residual acid solutions with or without Mb inhibitor. In fresh acid solution, a loose corrosion product film was formed on the surface of the substrate. When the Mb inhibitor appeared, the surface of

the substrate was relatively flat, and the trace of a polishing line could still be observed, which indicated that the presence of Mb inhibitor could effectively inhibit the corrosion behavior of HCl to casing steel, which was consistent with the weight loss method. At pH 1.0, a large number of streak-like corrosion products were formed on the surface of the substrate. Based on the EDS results in Table 3, it was determined that the main elements of the streak-like corrosion products were Fe, O, and C, which indicated that $FeCO_3$ might be formed on the substrate. When the Mb corrosion inhibitor appeared, a large number of spot-like corrosion products were detected on the substrate, and a small amount of streak-like corrosion products also appeared, but no traces of polishing lines were observed (Figure 6d). Under the condition of pH 3.0 without Mb (Figure 6e), stripe-like corrosion products also appeared on the substrate. Compared with the elemental composition of corrosion product film in areas A (Figure 6c) and B, it was determined that the content of C was higher under the condition of pH 3.0, which indicated that more $FeCO_3$ formed on the substrate with the increase in pH. In the solution containing a Mb inhibitor at pH 3.0, the corrosion products were covered on the surface of the substrate. It can be seen from Figure 6b,d,f that with the decrease in hydrogen ion concentration, more corrosion products are formed on the substrate.

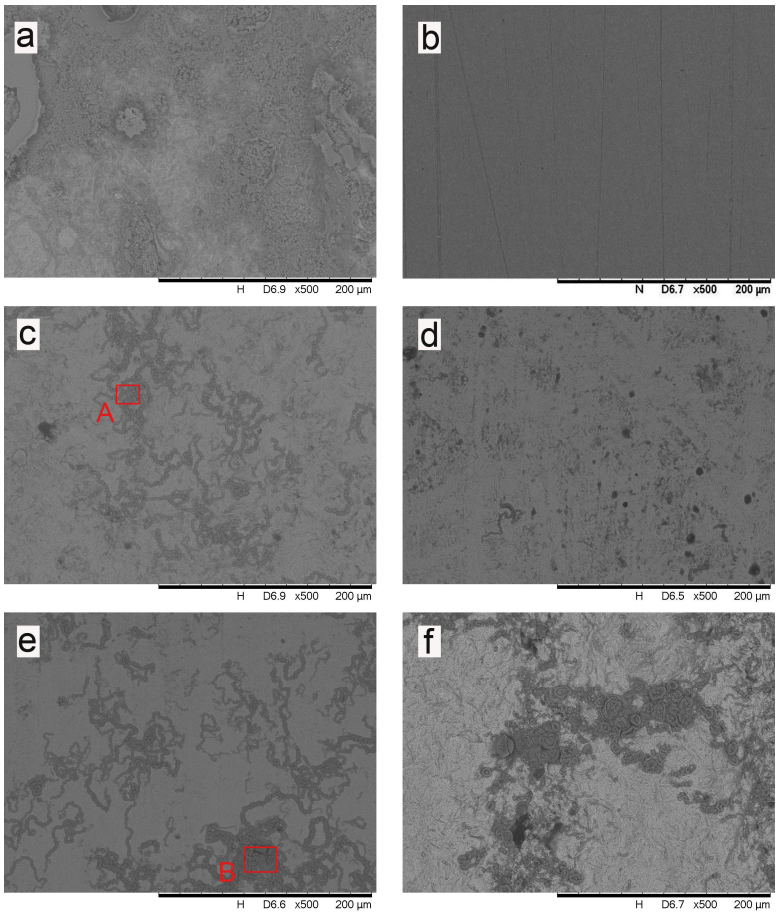


Figure 6. SEM of casing steel after being exposed to fresh and residual acid solutions with or without Mb inhibitor at 90 °C for 4 h: (**a**) 20% HCl; (**b**) 20% HCl + Mb; (**c**) pH 1.0; (**d**) pH 1.0 + Mb; (**e**) pH 3.0; (**f**) pH 3.0 + Mb.

Table 3. Elemental composition of the A and B regions (at.%).

Region	Fe	C	O	Cl
A	51.59	29.06	19.26	0.09
B	44.96	36.29	18.26	0.49

The elemental composition of the A (in Figure 6c) and B (in Figure 6d) regions are shown in Table 3.

3.4. 3D Profilometry

The 3D morphology results of the casing steel in the residual acid solution with or without Mb are shown in Figure 7. After removing the product film, the surface of the substrate was relatively flat in the residual acid without Mb. The corrosion type of casing steel was uniform corrosion under the condition of residual acid (Figure 7a,c). In the residual acid solution containing Mb at pH 1.0 (as shown in Figure 7b), pits were detected on the surface of the substrate, and the pitting rate reached 47.41 mm y^{-1}.

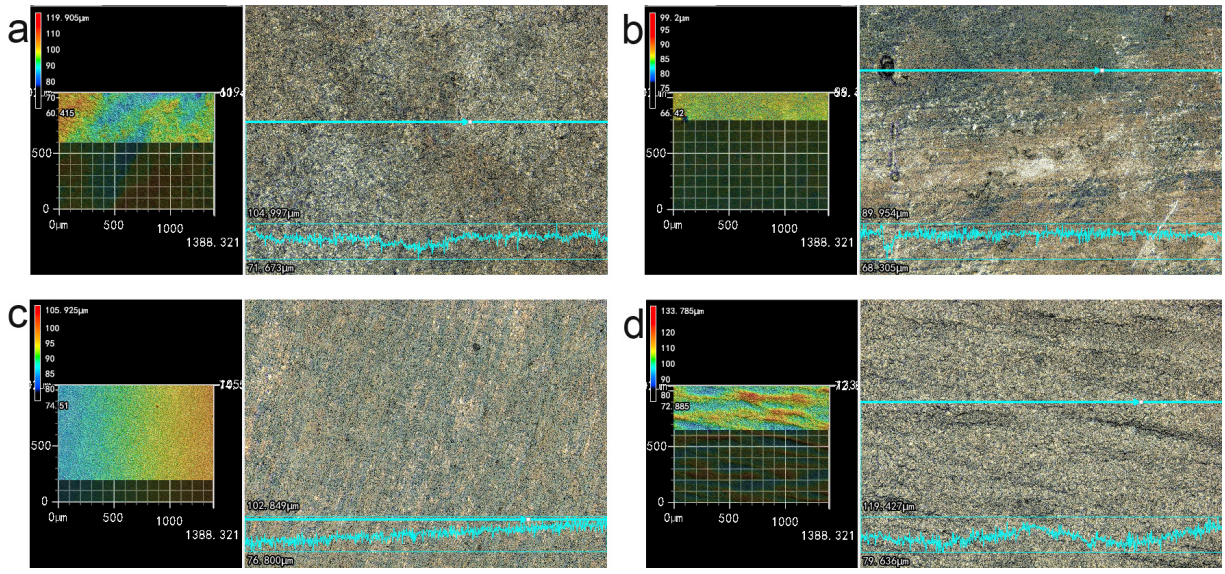


Figure 7. 3D profilometry of casing steel after exposed in residual acid solutions with or without Mb inhibitor for 4 h at 90 °C: (**a**) pH 1.0; (**b**) pH 1.0 + Mb; (**c**) pH 3.0; (**d**) pH 3.0 + Mb.

In the residual acid solution containing corrosion inhibitor at pH 3.0, although no pitting pits were observed on the substrate, the surface of the substrate was corrugated (Figure 7d), and the height difference between the peaks and troughs formed was close to 40 μm. The appearance of corrosion products might reduce the adsorption characteristics of corrosion inhibitors on the substrate so that the corrosion medium reacted with the substrate at the weak part of the adsorption film to form pits. The corrosion product morphology in Figure 6f combined with the 3D morphology in Figure 7d after removing the corrosion product film also supported this view.

3.5. XPS Analysis

The XPS results of C, O, Fe, and N elements of casing steel in hydrochloric acid solution with or without Mb at pH 3.0 are shown in Figure 8. The residual peak of C 1s at 284.6 eV was used to calibrate the binding energy of each substance. In the residual acid solution without Mb, the peak of C 1s, O 1s, and Fe $2p_{3/2}$ was at 288.0 eV, 531.4 eV, and 711.3 eV, respectively, indicating the appearance of $FeCO_3$ [21]. The peak of O 1s at 529.7 eV, the peak of Fe $p_{3/2}$ at 710.9 eV and 718.7eV, and the peak of Fe $2p_{1/2}$ at 724.5 eV corresponded to Fe_2O_3 [22]. When the Mb was added, the binding energy of C, O, and Fe elements was the same. In addition, the peak of N 1s was at 399.0 eV, which might be related to the residual Mb on the surface of the substrate or the corrosion products from the interaction between the Mb and the substrate.

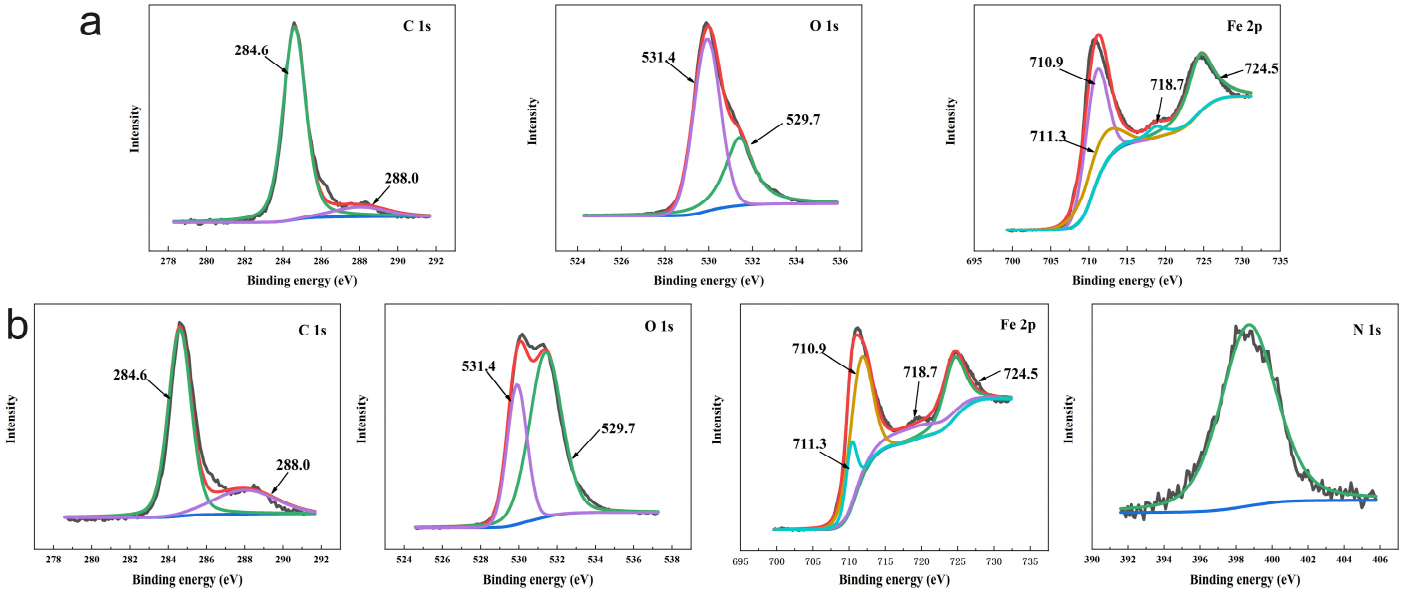


Figure 8. XPS results after immersion of casing steel in residual acid solution with or without Mb inhibitor at 90 °C for 4 h: (**a**) pH 3.0; (**b**) pH 3.0 + Mb.

4. Discussion

When no Mb was present, the morphology of corrosion products of casing steel in residual acid and the fresh acid solution was different (Figure 9a,b), which was mainly due to the addition of a large amount of $CaCO_3$ in the solution under the condition of residual acid. In the solution, CO_3^{2-} combines with Fe^{2+} to form $FeCO_3$ on the substrate, and the increase in solution pH value was beneficial to $FeCO_3$ film formation on the substrate, which was confirmed by the results of Figure 6c,e [23]. The increase in pH value of the solution led to the decrease in hydrogen concentration in the solution, which was the main reason for the significant difference in Tafel slope in the cathodic reaction process between residual acid and fresh acid. Moreover, the difference in corrosion product film protection between residual acid and fresh acid might affect the diffusion process of hydrogen ions, thus affecting the cathodic reaction process.

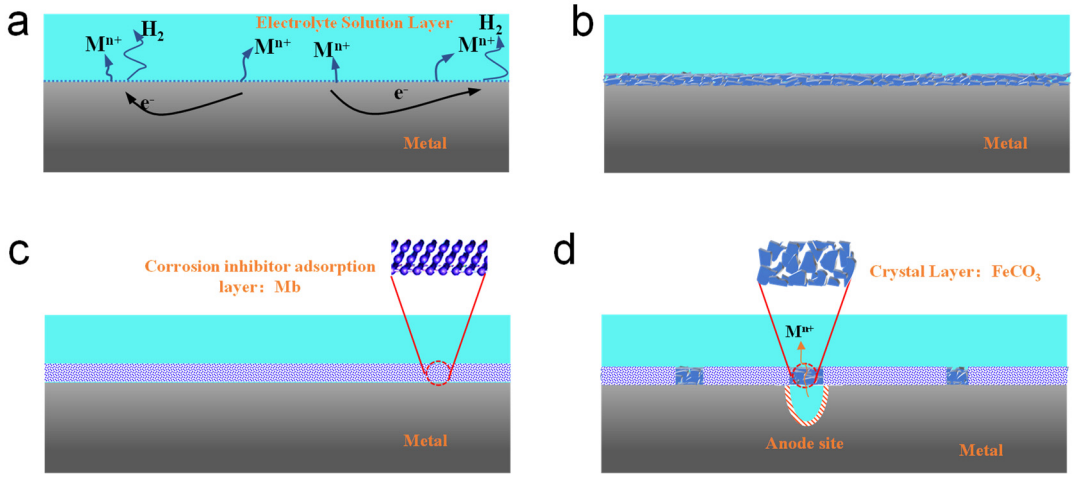


Figure 9. Corrosion/corrosion inhibition mechanism model diagram: (**a**) fresh acid; (**b**) residual acid; (**c**) fresh acid with Mb; (**d**) residual acid with Mb.

When Mb was added to fresh acid and residual acid solution, the decrease in corrosion rate occurred due to the adsorption of Mb molecules to the surface of the substrate to inhibit

the corrosion of casing steel (Figure 9c). The adsorption of Mb on carbon steel surface belonged to mixed adsorption, which was also supported by current electrochemical results [14]. The sharing electrons were formed between p-electrons of the heterocyclic ring and vacant d orbitals of surface iron, and the adsorption of Mb molecules and mild steel belonged to chemical adsorption. In addition, the aromatic ring in the Mb molecule can also be used as an electron donating functional group to promote the chemisorption with the steel. Mb molecule might undergo protonation reaction in residual acid solution to obtain protonated Mb with a positive charge. The reaction is shown in Formula (3):

$$C_{20}H_{22}N_3OCl + xH^+ \rightarrow [C_{20}H_{22+x}N_3OCl]^{x+}. \quad (3)$$

Because the hydration degree of Cl^- was small, Cl^- was conducive to the formation of excessive negative charge near the substrate, which promoted the electrostatic adsorption between protonated Mb and steel, which belonged to physical adsorption.

Under the condition of residual acid, the appearance of Mb promoted the local corrosion of casing steel (Figure 9d). There was a certain corresponding relationship between the 3D morphology of corrosion product film removed in Figure 7b,d and the distribution of corrosion product film on the substrate surface in Figure 6d,e. It could be inferred that the $FeCO_3$ corrosion product hindered the adsorption of the Mb inhibitor on the substrate. The Q_{dl} value in Table 2 under the condition of residual acid containing Mb was smaller than that under the condition of fresh acid containing Mb, which supported this point. The results showed that the coverage rate of Mb molecule in the area where $FeCO_3$ corrosion product film exists was reduced, and the $FeCO_3$ corrosion product film had a less protective effect on the substrate than the adsorption film formed by Mb. The corrosion medium could react with the substrate through the $FeCO_3$ corrosion product film, thus promoting the occurrence of local corrosion.

5. Conclusions

In the present work, we obtain the following conclusions:

(1) Compared with the residual acid, the Mb inhibitor had higher inhibition efficiency under fresh acid conditions.

(2) Under fresh acid and residual acid conditions, Mb promoted the increase in Ecorr, and increased the Tafel slope of cathode and anode, resulting in an increase in reaction resistance. Therefore, Mb inhibitor showed mixed inhibition.

(3) Local corrosion of casing steel occurred in a residual acid solution containing Mb inhibitor. The occurrence of localized corrosion was related to the decrease in Mb inhibitor coverage on the substrate surface and the poor protection of $FeCO_3$ film.

(4) The $FeCO_3$ corrosion product hindered the adsorption of the Mb inhibitor on the substrate. The corrosion medium could react with the substrate through the $FeCO_3$ corrosion product film, thus promoting the occurrence of local corrosion.

Author Contributions: Data curation, W.Y. and Z.M.; Methodology, Z.W. and J.Z.; Project administration, L.W. and W.Y.; Resources, C.L. and K.L.; Writing—original draft, Z.M., X.J. and. Z.X.; Writing—review & editing, Z.M., K.L. and W.Y. All authors have read and agreed to the published version of the manuscript.

Funding: This research was founded by the Opening project fund of Materials Service Safety Assessment Facilities, MSAF-2021-102.

Institutional Review Board Statement: Not applicable.

Informed Consent Statement: Not applicable.

Data Availability Statement: Data is contained within the article.

Conflicts of Interest: The authors declare no conflict of interest.

References

1. Lou, Q.; Du, W.; Han, X.; Liu, W.; Song, H. Study on the Mechanical Properties of 125S Casing for oil and gas wells. *J. Phys. Conf. Ser.* **2020**, *1605*, 012123. [CrossRef]
2. Li, Z.B.; Lu, L.; Bi, Z.Y.; Zhang, F.; Huang, X.J.; Liu, Y.M. Heat treatment process of Q125 grade SEW oil casing steel. *Cailiao Rechuli Xuebao/Trans. Mater. Heat Treat.* **2016**, *37*, 156–161.
3. Farrokhrouz, M.; Taheri, A.; Keshavarz, A. Numerical reactive flow transport simulation on core samples during acid fracturing in carbonaceous shale. *J. Nat. Gas Sci. Eng.* **2020**, *84*, 103615. [CrossRef]
4. Shen, C.; Alvarez, V.; Koenig, J.D.B.; Luo, J.-L. Gum Arabic as corrosion inhibitor in the oil industry: Experimental and theoretical studies. *Corros. Eng. Sci. Technol.* **2019**, *54*, 444–454. [CrossRef]
5. Zhang, K.; Chen, M.; Zhou, C.; Dai, Y.; Liu, F.; Li, J. Study of alternating acid fracturing treatment in carbonate formation based on true tri-axial experiment. *J. Pet. Sci. Eng.* **2020**, *192*, 107268. [CrossRef]
6. Zhang, R.; Hou, B.; Zhou, B.; Liu, Y.; Xiao, Y.; Zhang, K. Effect of acid fracturing on carbonate formation in southwest China based on experimental investigations. *J. Nat. Gas Sci. Eng.* **2020**, *73*, 103057. [CrossRef]
7. Sheng, M.; Khan, W.A.; Cheng, S.; Zhang, P.; Tian, S.; Xu, Q. Characteristics of micro-fracturing in shales induced by dilute acid. *J. Nat. Gas Sci. Eng.* **2021**, *88*, 103855. [CrossRef]
8. Kumar, H.; Yadav, V. Highly efficient and eco-friendly corrosion inhibitor for mild steel in 5 M HCl: An anti-pitting and anti-cracking agent. *Chem. Data Collect.* **2020**, *30*, 100552. [CrossRef]
9. Yadav, M.; Sharma, D.; Sarkar, T.K. Adsorption and corrosion inhibitive properties of synthesized hydrazine compounds on N80 steel/hydrochloric acid interface: Electrochemical and DFT studies. *J. Mol. Liq.* **2015**, *212*, 451–460. [CrossRef]
10. Akalezi, C.O.; Maduabuchi, A.C.; Enenebeaku, C.K.; Oguzie, E.E. Experimental and DFT evaluation of adsorption and inhibitive properties of *Moringa oliefera* extract on mild steel corrosion in acidic media. *Arab. J. Chem.* **2020**, *13*, 9270–9282. [CrossRef]
11. Lin, B.-L.; Shao, J.-J.; Xu, Y.-Y.; Lai, Y.-M.; Zhao, Z.-N. Adsorption and corrosion of renewable inhibitor of *Pomelo* peel extract for mild steel in phosphoric acid solution. *Arab. J. Chem.* **2021**, *14*, 103114. [CrossRef]
12. Zafari, S.; Sarabi, A.A.; Movassagh, B. A novel green corrosion inhibitor based on task-specific benzimidazolium ionic liquid for carbon steel in HCl. *Corros. Eng. Sci. Technol.* **2020**, *55*, 589–601. [CrossRef]
13. Ayeni, A.O.; Akinyele, O.F.; Hosten, E.C.; Fakola, E.G.; Olalere, J.T.; Egharevba, G.O.; Watkins, G.M. Synthesis, crystal structure, experimental and theoretical studies of corrosion inhibition of 2-((4-(2-hydroxy-4-methylbenzyl)piperazin-1-yl)methyl)-5-methylphenol—A Mannich base. *J. Mol. Struct.* **2020**, *1219*, 128539. [CrossRef]
14. Ahamad, I.; Prasad, R.; Quraishi, M.A. Adsorption and inhibitive properties of some new Mannich bases of Isatin derivatives on corrosion of mild steel in acidic media. *Corros. Sci.* **2010**, *52*, 1472–1481. [CrossRef]
15. Ferkous, H.; Djellali, S.; Sahraoui, R.; Benguerba, Y.; Behloul, H.; Çukurovali, A. Corrosion inhibition of mild steel by 2-(2-methoxybenzylidene) hydrazine-1-carbothioamide in hydrochloric acid solution: Experimental measurements and quantum chemical calculations. *J. Mol. Liq.* **2020**, *307*, 112957. [CrossRef]
16. Pan, Y.; Zhan, F.T.; Yang, Z. Effect of Carbon Chain Length of Hydrophobic Group of Mannich Bases on Their Corrosion Inhibition Performance. *Mater. Prot.* **2015**, *48*, 23–25+50. [CrossRef]
17. Guo, H.; Dong, X.; Yang, J.; Xu, X. Synthesis and performance evaluation of double Mannich base acidizing corrosion inhibitor. *Mod. Chem. Ind.* **2020**, *40*, 180–184. [CrossRef]
18. *ASTM G1-03(2017)e1*; Standard Practice for Preparing, Cleaning, and Evaluating Corrosion Test Specimens. ASTM Standard: Philadelphia, PA, USA, 2017; pp. 1–9. [CrossRef]
19. *ASTM G31-72(2004)*; Standard Practice for Laboratory Immersion Corrosion Testing of Metals. ASTM Standard: Philadelphia, PA, USA, 2004; pp. 1–8. [CrossRef]
20. Ferreira, E.S.; Giacomelli, C.; Giacomelli, F.C.; Spinelli, A. Evaluation of the inhibitor effect of l-ascorbic acid on the corrosion of mild steel. *Mater. Chem. Phys.* **2004**, *83*, 129–134. [CrossRef]
21. Tang, Y.; Guo, X.P.; Zhang, G.A. Corrosion behaviour of X65 carbon steel in supercritical-CO_2 containing H_2O and O_2 in carbon capture and storage (CCS) technology. *Corros. Sci.* **2017**, *118*, 118–128. [CrossRef]
22. Heuer, J.K.; Stubbins, J.F. An XPS characterization of $FeCO_3$ films from CO_2 corrosion. *Corros. Sci.* **1999**, *41*, 1231–1243. [CrossRef]
23. Guo, S.; Xu, L.; Zhang, L.; Chang, W.; Lu, M. Corrosion of alloy steels containing 2% chromium in CO_2 environments. *Corros. Sci.* **2012**, *63*, 246–258. [CrossRef]

Disclaimer/Publisher's Note: The statements, opinions and data contained in all publications are solely those of the individual author(s) and contributor(s) and not of MDPI and/or the editor(s). MDPI and/or the editor(s) disclaim responsibility for any injury to people or property resulting from any ideas, methods, instructions or products referred to in the content.